

# The representation of Shallow cumulus convection and associated cloud fields in the Rossby Centre Atmospheric Model (RCA).

Colin Jones<sup>1</sup> and Enrique Sanchez<sup>2</sup>

<sup>1</sup>Rosby Centre SMHI, Norrköping

<sup>2</sup>INM, Madrid

email : [Colin.Jones@smhi.se](mailto:Colin.Jones@smhi.se)

## 1. Introduction and Motivation

Shallow cumulus convection is known to play a key role in determining the thermodynamic structure of the subtropical oceanic boundary layer. Transport of moisture associated with shallow cumulus clouds, is the primary water source balancing subsidence drying at the top of the subtropical PBL. Maintenance of a warm, moist subtropical oceanic boundary layer is crucial in the downstream development of deep cumulus convection.

Shallow convection also plays a fundamental role in the extra-tropics. Ubiquitous shallow convective clouds are often observed behind cold fronts, embedded within synoptic disturbances, over the extra-tropical oceans. The atmospheric warming induced by this mixing, located predominantly in the cold sector of the low pressure system, will act to reduce the thermal gradients from which the system derives its energy. As a result shallow cumulus convection may play a role in the energetics of extra-tropical low pressure systems, reducing their intensity slightly.

Over land in the extra-tropics, shallow convection occurs regularly on summer afternoons. Mixing in these cumulus clouds, acts to produce a well mixed boundary layer that deepens through the afternoon into the early evening. A typical cloud field associated with shallow convection will often be non-precipitating and cover around 10-30% of the sky. As shallow convective clouds often develop in the middle of a summer afternoon, they interact strongly with the incoming solar radiation field. As a result, they modify the surface radiation flux and directly affect the surface temperature and soil moisture fields. The details of the thermodynamic structure of the planetary boundary layer, left at the end of the day after shallow convection, determines the likelihood for the presence or absence of nocturnal clouds. Through interaction with the terrestrial long wave radiation field the presence or not of clouds can also influence nocturnal surface temperatures. Finally, shallow convection is often a precursor to the development of precipitating, deep cumulus convection and may play a role in determining the typical onset time for this type of convection over summertime continental land masses, namely the evening-early night time.

Due to the subtle physics occurring in the development of shallow cumulus convection, numerical models often have great difficulty accurately representing this type of convection (For a detailed discussion of shallow convective mixing see Emanuel 1994 and Betts 1997). It is very easy for models to misrepresent the development of shallow convection and develop one of the following erroneous atmospheric states:

- (i) A dry well mixed boundary layer
- (ii) A stratocumulus topped boundary layer, typically with 100% cloud cover.
- (iii) A field of precipitating deep convective clouds.

Atmospheric state (i) will lead to an over prediction of the surface radiation flux, state (ii) will cause a gross underestimate of the surface radiation flux and state (iii) will give incorrect precipitation amounts. If these errors are systematic (which they often are), when models are run in climate mode, serious errors can develop in the seasonal mean surface temperature, soil moisture and precipitation. These types of errors can also lead to NWP forecast failures, particularly related to surface radiation and precipitation. Even if models successfully simulate the development of shallow cumulus convection, to simulate the correct cloud-radiation interaction requires accurately modelling the cloud field associated with the shallow cumulus mixing, and its timing in the solar day. This is quite a stringent test of an atmospheric model.

Clearly, it is extremely important that climate and weather forecast models accurately represent the temporal evolution of shallow cumulus convection and the thermodynamic and radiative effects associated with this type of convection. In this communication, I analyse the representation of extra-tropical, land based, summertime shallow convection in the RCA model. I consider the timing of onset and subsequent development of shallow convection within the solar day. I further analyse the thermodynamic and cloud fields associated with this shallow convection and imply the impact of the clouds on the surface solar radiation. I will introduce a new method for parameterising the cloud fraction associated with shallow convection in RCA. This method is felt to be physically more consistent and produces results at least comparable to the original RCA treatment of shallow cumulus cloud fraction. I will further show that the surface radiation flux is sensitive to the details of how one models the shallow cumulus cloud fraction and associated incloud microphysics.

## **2. Experimental Design.**

To isolate the representation of shallow cumulus convection within the RCA model, a single column version of RCA was integrated for a typical shallow cumulus day over the Southern Great Plains Atmospheric Radiation Measurement site (ARM SGP) in Oklahoma (<http://www.arm.gov>). The model was initialised at 11.30a.m. UTC (5.30 local time) on June 21<sup>st</sup> 1997 and integrated for a 14.5 hour period. Large scale advective and radiative tendencies were externally prescribed from a mixture of observations and radiative transfer models, with the resulting tendency terms passed through a variational assimilation scheme. Surface forcing was smoothly prescribed from high temporal resolution observations at the ARM SGP site. (More details of the prescribed forcing can be found in Brown etal (2001) and at <http://www.knmi.nl/samenw/eurocs>). Integrating the single column model with prescribed surface, radiative and large scale advective forcing allows the model parameterisations of turbulence, convection and cloud processes to be evaluated in isolation. These single column integrations form part of an EU Framework V project EUROCS (see <http://www.cnrm.fr/eurocs> for more details on EUROCS). Several single column models were integrated for this test day within the EUROCS project. Results of these models, including the HIRLAM reference model, can be found at the aforementioned www sites. A number of Large Eddy Simulation Models (LES Models) have also been integrated with the same large scale and surface forcing. LES models explicitly resolve the cloud scale and boundary layer turbulence associated with shallow cumulus convection. Brown etal (2001) have documented the high quality of the contributing LES models for this case. Results from the single column models can therefore be compared directly to high quality observations at the ARM SGP site and with LES models. Comparison with LES models allows a degree of verification of processes that are not amenable to observation but which are, nevertheless, key processes to

parameterise in shallow cumulus convection (e.g cloud mass flux, entrainment and detrainment rates into and out of cumulus clouds).

### 3. Model Description

The RCA model uses a prognostic turbulent kinetic energy (TKE) scheme to parameterise subgrid scale vertical fluxes in the free atmosphere, the CBR scheme (Cuxart et al 2000), as used in the HIRLAM reference model. Deep and shallow convection uses the parameterisation due to Kain and Fritsch 1990. The large scale cloud fraction is parameterised as a function of the excess grid box mean relative humidity, beyond a critical threshold defined for the onset of clouds (Slingo 1987). Cloud fraction associated with active convective turrets is a direct function of the convective mass flux and follows the ideas of Xu and Kruger (1991). Finally the large scale cloud microphysical and precipitation production parameterisation is described in Rasch and Kristjansson (1998). A more complete discussion of the parameterisation schemes in the RCA model are presented in Jones (2001). The interested reader is referred to this or the aforementioned references for an in depth discussion. Here I will highlight the key parts of the schemes with respect to the representation of shallow cumulus convection and associated cloud fields.

The Kain Fritsch scheme is a bulk cloud model parameterisation of cumulus convection. A single active updraft and, for deep convection only, a single active downdraft are modelled. Entrainment and detrainment into/out of the plumes is based on the concept of buoyancy sorting (Blyth 1988, Emanuel 1994), whereby negatively buoyant admixtures of cloud and environmental air detrain into the environment and positively buoyant admixtures entrain into the cloud and increase the cloud mass flux. Prior to entering the convection scheme, model vertical columns are tested for their ability to support convection. Convection is only tested for if upward vertical motion or a TKE value greater than  $0.25\text{kgm}^2\text{s}^{-2}$  is found in the column, somewhere within 500hpa of the surface. Due to frequent weak large scale subsidence in shallow convective regions, this can often mean shallow convective activity is directly controlled by the amount of lower tropospheric TKE. Once a vertical column enters the convection scheme, the thermodynamic properties of a 50hpa thick layer of air, whose base is at the lowest model level, is calculated and tested for its ability to support deep convection. The requirements for deep convection are; (i) positive CAPE (Convective Available Potential Energy) exists in the column, (ii) the 50hpa thick layer when lifted to its LCL (Lifting Condensation Level) satisfies a specific convective trigger function, (iii) after satisfying the trigger function the parcel must be able to build a cloud of depth 2-3km (the details being a function of the parcel temperature at the LCL).

The trigger function, which is applied both to deep convection and subsequently shallow convection, is described in Fritsch and Chappell (1980). Essentially, it requires that the lifted 50hpa parcel is buoyant at its LCL. A temperature perturbation is added to the parcel temperature at the LCL, if the large scale vertical motion is upward. This is to mimic the fact that in a field of large scale ascent there is a degree of spatial variability in the plume buoyancy field, with some plumes being more buoyant than the grid box mean value. The grid scale vertical velocity field is translated into a temperature perturbation and added to the plume temperature at the LCL. A further temperature perturbation is applied to the parcel if the grid box mean relative humidity at the LCL lies between 0.75-0.95. This perturbation simulates the spatial variance in the relative humidity field, in that some portion of the model grid box may be at saturation if the grid box mean relative humidity is high.

The trigger function is schematically written as:

$$\mathbf{T(parcel)_{LCL} + T(pert)_{\omega} + T(pert)_{RH} > T(env)_{LCL}}$$

Where T represents the virtual temperature.

$$\mathbf{T(pert)_{\omega} = C_0 \omega^{0.33}}$$

$$\mathbf{T(pert)_{RH} = 0.25(RH_{LCL} - 0.75) * Q_{MIX} * \partial(q_s)/\partial t \quad (0.75 < RH_{LCL} < 0.95)}$$

$$\mathbf{T(pert)_{RH} = (1/RH_{LCL} - 1) * Q_{MIX} * \partial(q_s)/\partial t \quad (RH_{LCL} > 0.95)}$$

Here  $Q_{mix}$  is the 50hpa parcel mean mixing ratio and  $dq_s/dt$  is the tendency of  $Q_{mix}$  as the parcel is lifted to its LCL.  $C_0$  is a scaling parameter that scales the vertical velocity perturbation as a function of the model resolution. The scaling parameter attempts to provide a similar temperature perturbation as resolution varies due to the varying nature of  $\omega$ , the resolved vertical velocity, with resolution.

If this 50hpa parcel does not satisfy these three criteria then it is deemed unable to support deep convection. A new 50hpa layer, with base at the 2<sup>nd</sup> lowest model level, is now tested for convection. This procedure is applied through the lowest 800hpa of the model atmosphere or up to 200hpa, whichever occurs first. If no parcels satisfy these three criterion then the vertical column cannot support deep convection and shallow convection is tested for. In testing for shallow convection the same trigger function is applied as for deep convection. But now positive CAPE is not required in the grid column and a cloud of any vertical extent is allowed. Parcels are tested from the lowest model layer again, but now are assumed to be only 25 hpa thick, with a new, representative mean thermodynamic state calculated. If the trigger function cannot be satisfied or no ascending cloudy plumes are buoyant then the test for shallow convection also fails. If a parcel can ascend through 2 model layers and form a cloud of some depth then shallow convective mixing is allowed to ensue. The closure term determining the degree of shallow convective mixing is directly proportional to the maximum amount of TKE in the planetary boundary layer. The closure term, along with the rates of entrainment and detrainment into and out of the ascending plume and the assumed cloud radius of 300m, determine the final shallow convective cloud depth and updraft mass flux in the cloud. Through compensatory subsidence and detrainment the cloud mass flux determines the tendency terms of temperature, mixing ratio and cloud water due to shallow convective mixing.

In the original formulation of shallow convection in the RCA model, there was no formal parameterisation of a shallow convective cloud fraction. The convection scheme provided tendency terms of temperature, mixing ratio and cloud water. All cloud water was assumed to detrain into the environment and was evaporated as a function of the grid scale relative humidity. A cloud fraction, associated with shallow convection, was calculated through the large scale cloud fraction parameterisation. This means that any shallow convective cloud fraction is a function solely of the local grid box mean relative humidity. It also means that these clouds only form where and when the relevant relative humidity thresholds, in the large scale cloud fraction scheme, are exceeded. These thresholds have been developed primarily for typical large scale cloud fields and are by no means optimal for shallow convective clouds. With this in mind an alternative parameterisation of shallow convective cloud fraction has been tested on this case. The scheme is described in Albrecht (1981). In this scheme the

cloud field, associated with shallow convection, is made a function of both the local grid box relative humidity and the total water content of the shallow convective plumes. In this way the shallow convective cloud fraction is directly tied to the subcloud layer thermodynamic state, this determining the water content of the shallow cumulus updrafts. The resulting shallow convective cloud water, generated in the convection scheme, is now retained in the shallow cumulus cloud fraction determined via the Albrecht scheme. Cloud microphysical and precipitation processes are subsequently applied to this shallow cumulus cloud water field in a manner identical to that applied for large scale clouds. In this way, the entire shallow cumulus water cycle is tied more tightly to the parameterisation of shallow convective mixing and the cloud microphysical and cloud-radiative effects of the shallow convective clouds are more directly linked to the subcloud layer thermodynamics and shallow cumulus activity.

#### 4. Results and Discussion

The standard model set up described in this section will be that whereby the Albrecht cloud scheme is used for parameterising the shallow convective cloud fraction (referred to as RCA\_Albrecht). I will briefly contrast this with the original RCA model, in which the only difference is that shallow convective cloud fraction and subsequent incloud microphysics are calculated by the large scale cloud parameterisation scheme.

Figure 1 shows the evolution of the single column model Liquid Water Path (LWP), maximum cloud fraction and cloud top height, through the day. The model was initialised at 5.30am local time and integrated to 20.00 local time. For comparison, results from the KNMI Large Eddy simulation model (see <http://www.knmi.nl/samenw/eurocs> for details) are also plotted. Brown et al. (2001) indicate the degree of agreement between various LES models and observations, suggesting the LES model results can be used as a first order measure of the truth. In Figure 1A one can see that the diurnal variation of the LWP is well captured by the RCA model. Shallow cumulus activity starts slightly later than seen in the LES model but tends to decay late in the day around 18.00 as is seen in the LES results. The maximum values in RCA are higher than in the LES. There is a tendency for this in many of the contributing single column models (see <http://www.knmi.nl/samenw/eurocs> for this). At present, the absolute quality of the LES LWP field versus observations has not been formally documented. Nevertheless, the RCA model results are of the same order of magnitude as the LES results, this is encouraging. Figure 1B illustrates the maximum cloud fraction found in a single vertical layer, in the LES and RCA single column model. For RCA the convective cloud and large scale cloud fraction are plotted separately. In this case convective cloud always refers to the shallow cumulus cloud fraction diagnosed by the Albrecht scheme. If a shallow convective cloud fraction is diagnosed at a particular grid box, a large scale cloud is precluded from occurring at that point for the period a shallow convective cloud is present. The maximum convective cloud amount is of a similar magnitude to that diagnosed in the LES model, being ~10-15% of the total sky. The overall diurnal cycle of the 2D cloud fraction is not particularly well captured by the RCA model. In particular the Albrecht cloud scheme may need further tuning, nevertheless, the magnitude of the diagnosed cloud amounts are realistic. This parameter is extremely difficult to model and there is considerable scatter amongst the contributing single column models.

After 18:00 one can see a large scale cloud develop in figure 1B. From figure 1A it can be seen that this cloud contains very little cloud water making it fairly unimportant from a radiative perspective. This large scale cloud develops in a single layer at the top of the well mixed subcloud layer (not shown). At this level, vertical mixing through the day has

moistened the model atmosphere sufficiently to take the grid box mean relative humidity beyond the threshold for large scale clouds to form. Figure 5 (bottom row) indicates the relative humidity at the top of the subcloud layer is not greatly different from that seen in the LES results. The development of this cloud layer, late in the day, points more to problems in representing clouds with only relative humidity as a parametric term, rather than problems related to the shallow cumulus mixing in RCA. Figure 1C shows that the depth of shallow cumulus mixing and associated cloud depth is very realistically modelled through the diurnal cycle. Shallow cumulus mixing progressively deepens through the day producing a cloud top of ~3000 metres by the mid-afternoon.

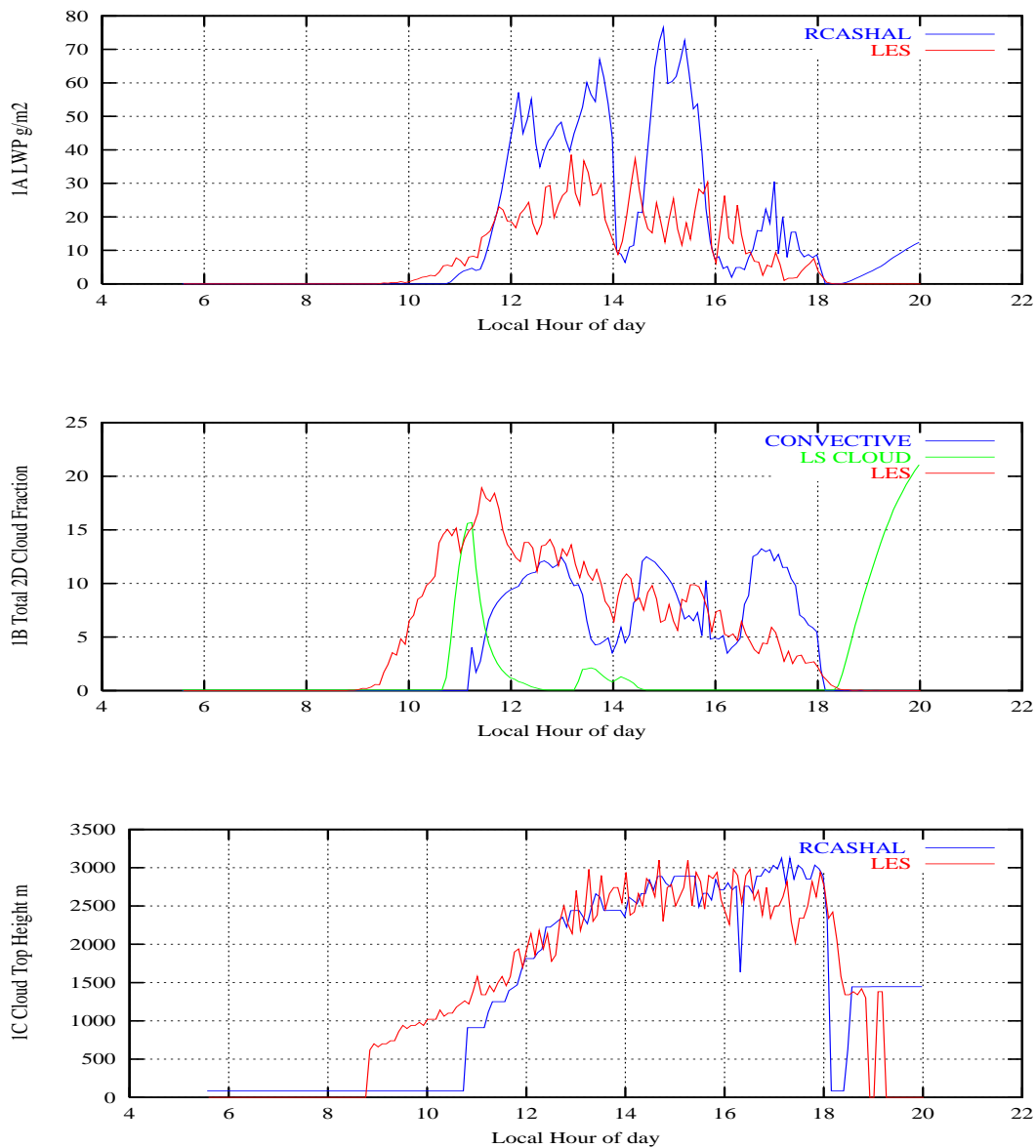


Figure 1: Diurnal Cycle of the simulated shallow cumulus cloud field, in the RCA single column model, using the Albrecht shallow cumulus cloud fraction scheme. A) Liquid Water Path in g/m<sup>2</sup> (Blue is RCA, Red is KNMI\_LES). B) Maximum cloud fraction (Blue is RCA convective cloud fraction, Green is RCA large scale cloud fraction and Red the KNMI\_LES cloud fraction). C) Cloud top height in metres. Time is local hour of day, values are 5 minute means.

Figure 2 contrasts the standard RCA results for this day, using the Albrecht shallow cumulus cloud scheme, to an RCA simulation where shallow cumulus cloud fraction was diagnosed through the large scale cloud scheme. In the latter, shallow cumulus cloud fraction is a function solely of relative humidity. All other aspects of the model are identical in the two simulations. While the diagnosed cloud fractions and cloud depth show a similar development, the liquid water paths are radically different. As a result, the radiative effect of the shallow cumulus clouds will be different in the two simulations. It is too early to say which simulation is the better, further evaluation against observations and more cases are needed.

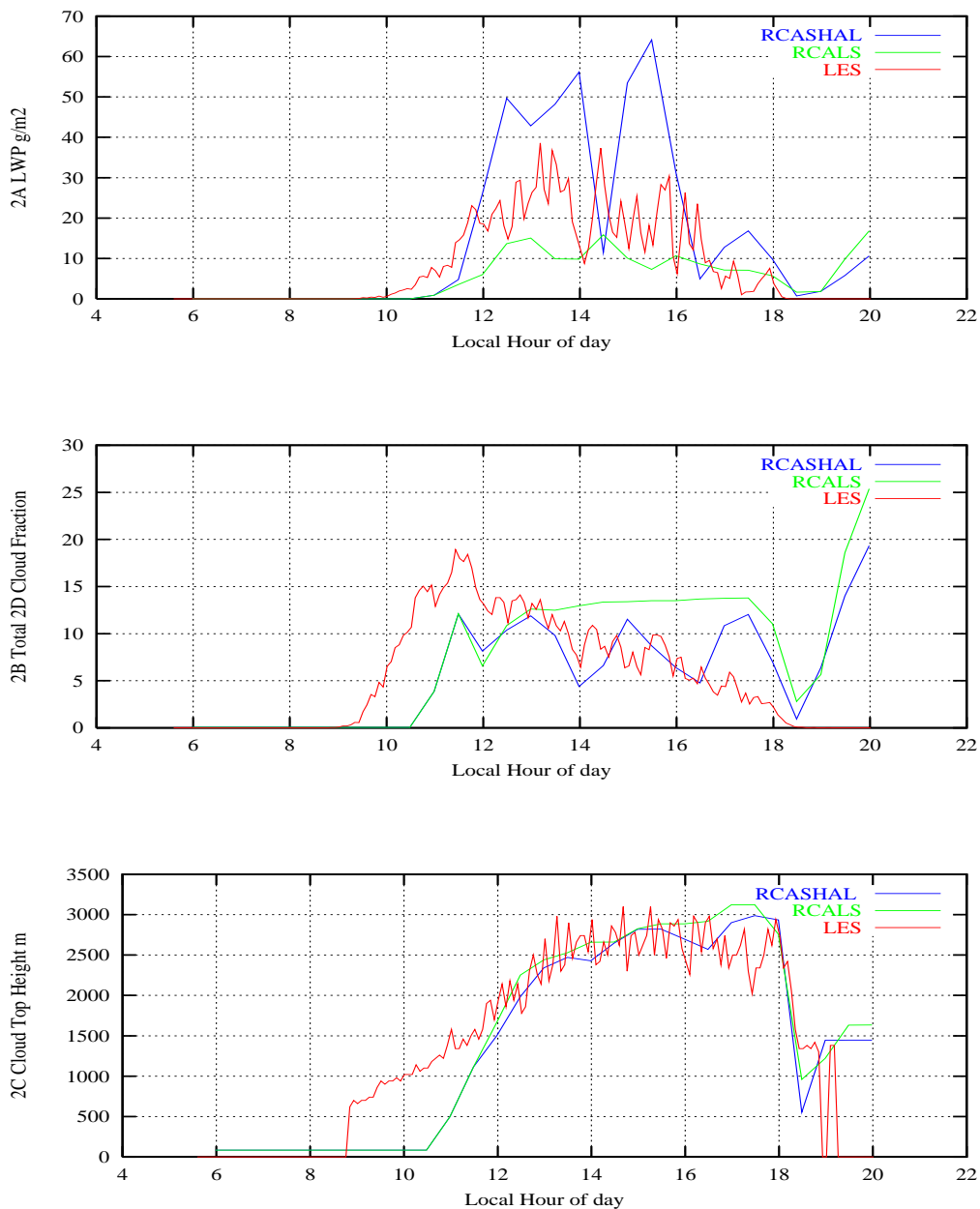


Figure 2. Comparison of the (A) LWP, (B) Maximum Cloud Fraction and (C) Cloud Top height. Blue curves show results from RCA with Albrecht Cloud Scheme. Green is RCA plus large scale cloud scheme for shallow cumulus cloud fraction. Red is KNMI\_LES results. Units are as in Figure 1. RCA results are 30 minute means.

Figure 3 illustrates the effect of the modelled shallow cumulus clouds on the surface solar radiation budget, for this day over the ARM SGP site. Figure 3A shows the effect on the surface solar radiation flux of the shallow cumulus clouds simulated by the standard RCA model with the Albrecht cloud scheme active. In this simulation the RCA radiation scheme was integrated twice every timestep. The first radiation calculation used the full evolving atmospheric state with the diagnosed cloud and cloud water amounts shown in figure 1. A resulting surface radiation flux was calculated with the full radiative effect of the shallow cumulus clouds felt by the RCA radiation code. Due to the application of prescribed surface fluxes and atmospheric radiative tendency terms, the calculated surface radiation flux is purely diagnostic and does not influence directly the model simulation. In the second call to the radiation code, the same atmospheric state was used but the cloud water amounts were set to zero. The resulting surface radiation flux can be considered the clear sky equivalent of the first radiation calculation. Differencing the two surface solar radiation fluxes, calculated every timestep, gives the effect of the shallow cumulus clouds on the surface solar radiation flux. It is this difference field that is plotted in figure 3A. In the middle of the day the modelled shallow cumulus clouds reduce the surface solar radiation flux, simulated by the RCA radiation code, by up to  $80\text{Wm}^{-2}$ . The mean effect across the entire day is some  $30\text{-}40\text{Wm}^{-2}$ , a significant impact on the surface solar flux. This flux difference will impact directly on the surface temperature and soil moisture in a fully prognostic model and must be accurately modelled. Systematic errors in the representation of the radiative effect of shallow cumulus clouds can clearly lead to serious surface solar radiation flux errors in climate models.

Figure 3B shows the difference in the diagnosed surface solar radiation flux between the experiment using the Albrecht cloud scheme and that where shallow cumulus clouds are diagnosed by the RCA model large scale cloud scheme. Differences of up to  $20\text{Wm}^{-2}$  can occur through the day. As can be seen in Figures 3C and D, these differences primarily result from the different liquid water paths in the simulated cloud fractions, the latter being rather similar. Clearly, models need a good simulation of the shallow cumulus mixing, the resulting cloud fraction and the incloud water amounts to accurately model the radiative effects of shallow cumulus clouds.

Aswell as assessing the temporal evolution of single level cloud fields in the RCA simulation, it is important to evaluate the evolving vertical structure of the shallow cumulus clouds and the model thermodynamic state. The vertical structure of the RCA simulation made with the Albrecht shallow cumulus cloud scheme, will be presented in this section. Figure 4 illustrates the evolution of the RCA model thermodynamic state through the day. Comparison to the KNMI LES model is again made. The top panel in figure 4 shows the evolution of the potential temperature field in the RCA model and KNMI\_LES model. Also shown is the initial profile at 5.30am. Profiles are plotted at 11.30, 14.30 and 17.30. The RCA results are 10 minute mean values, centred on the quoted time point. The middle panel shows the total water profiles at the same times and the bottom panel the relative humidity profiles. Again we are using the LES results as some measure of the truth. As discussed in Brown et al (2001), due to the difficulties in accurately prescribing the large scale and surface forcing, it is very difficult to compare single column and LES models directly to observations. As the LES models used the same forcing as prescribed for the RCA single column model we feel it more appropriate to compare the RCA results directly with the LES results. Brown et al further indicate that the inter-model differences in the thermodynamic profiles, between contributing LES models, is very small. We therefore view the KNMI\_LES results as fairly representative of all LES models.

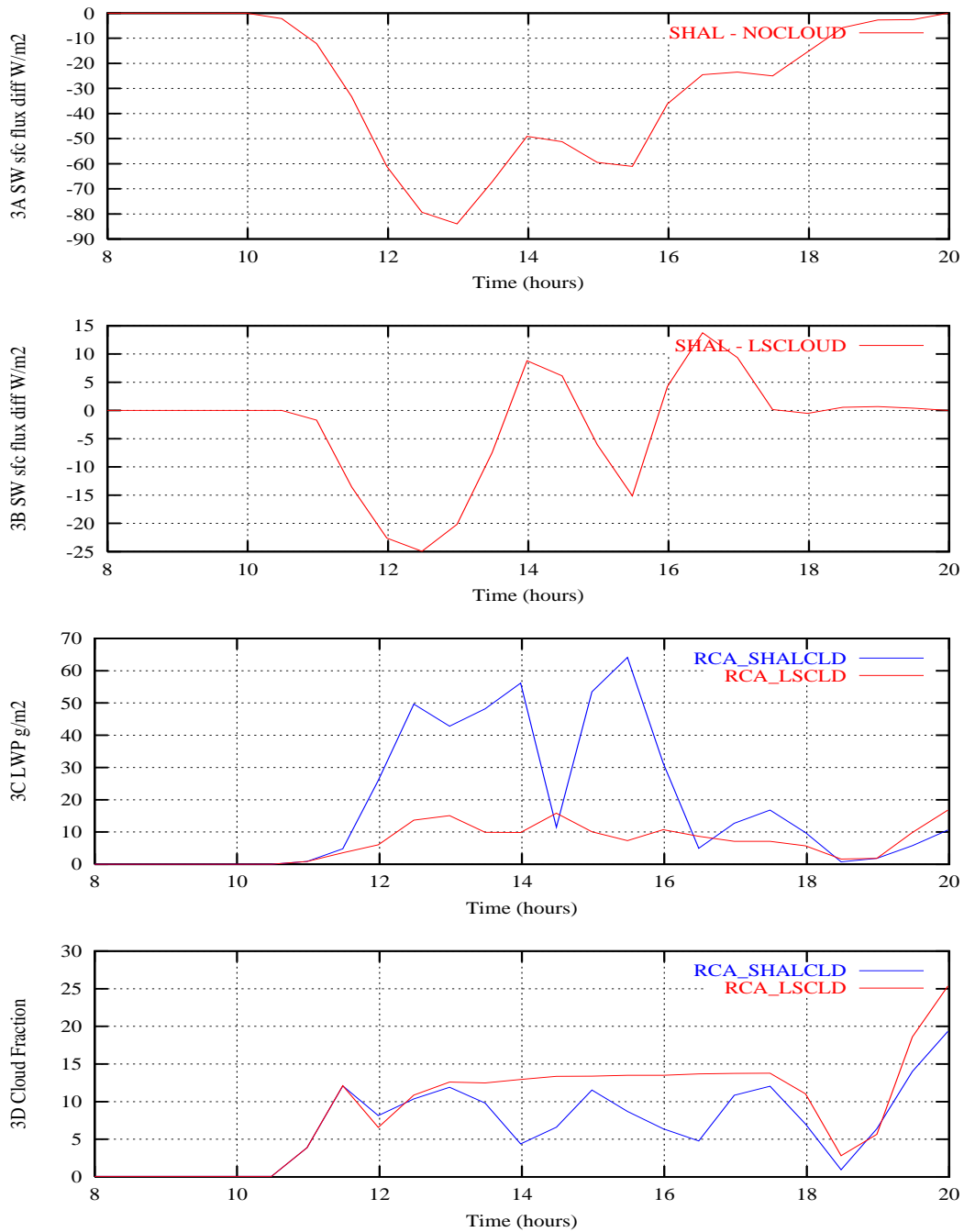


Figure 3A. Surface shortwave solar radiation flux difference ( $W/m^2$ ) produced by the shallow cumulus cloud field in figure 1 minus the surface radiation flux for an equivalent clear sky. Figure 3B surface shortwave solar flux difference between RCA\_Albrecht minus RCA\_lscloud experiment. Figure 3C shows the LWP field in the RCA\_Albrecht (Blue) and RCA\_lscloud (Red) experiments and figure 3D the maximum cloud fraction in the respective experiments.

The evolution of the potential temperature profile, through the simulated day, appears very accurate in RCA when compared to the LES model. A deepening, well mixed profile is seen to evolve through the day. The RCA model appears to mix too deeply when compared to the LES model. This tendency can also be seen in the evolution of the total water and relative humidity profiles. We will indicate later that this is probably a result of some assumptions

made in the convection scheme related to the parameterisation of entrainment and detrainment and the specification of a single shallow cumulus cloud radius. The total water also shows a deepening, well mixed boundary layer and the shallow convective transport of water substance into the free atmosphere, above ~1500m. Again, RCA appears to transport water to higher levels than the LES results indicate, with significant moistening above 2500m compared to the initial profile. This can also be seen in the relative humidity profiles, with a dry bias in the lower cloud layer, between 1000-2000 metres and a moist bias above ~2000 metres compared to the LES results. Below 1000 metres the evolution of the relative humidity profile is well simulated by RCA.

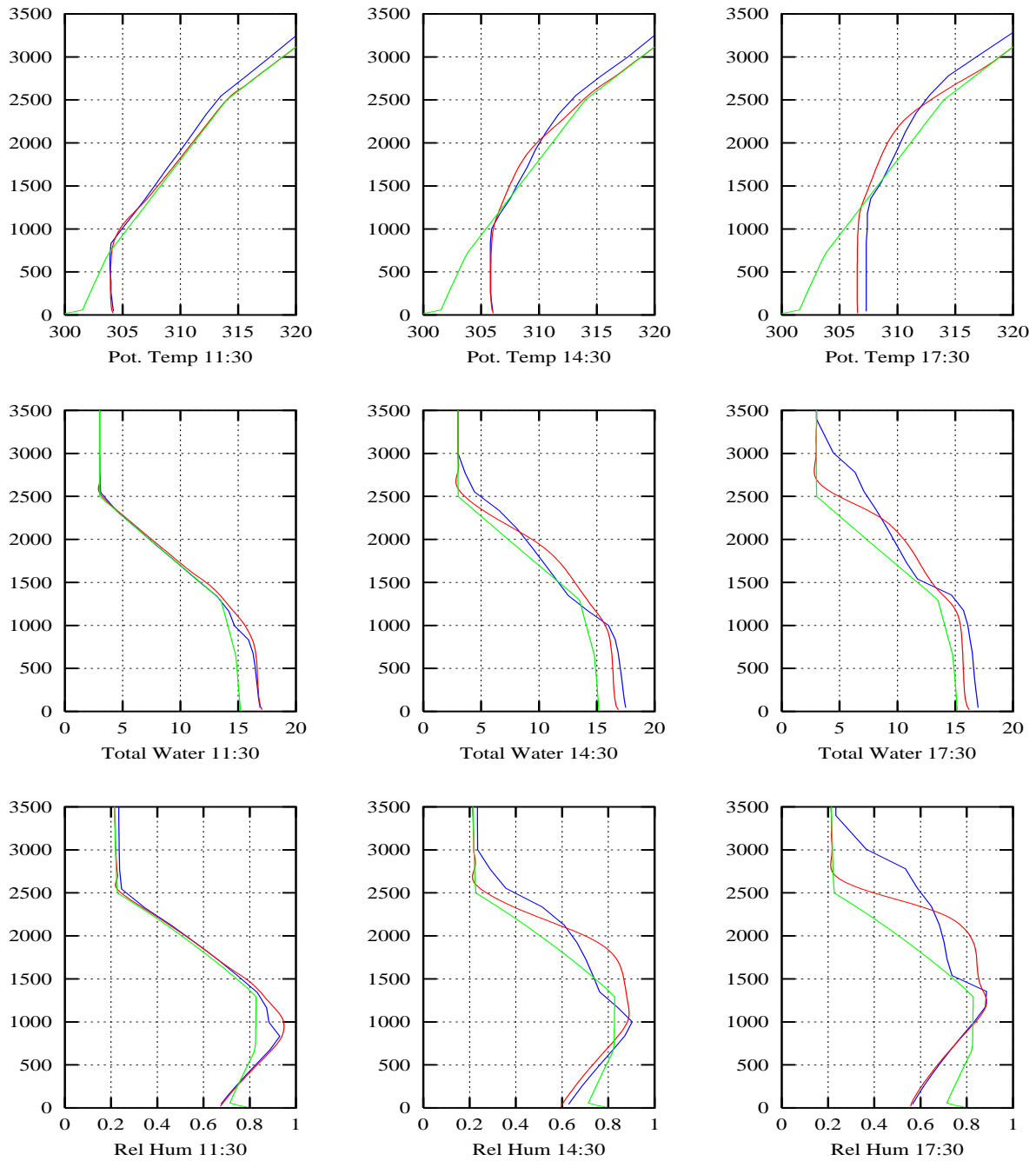
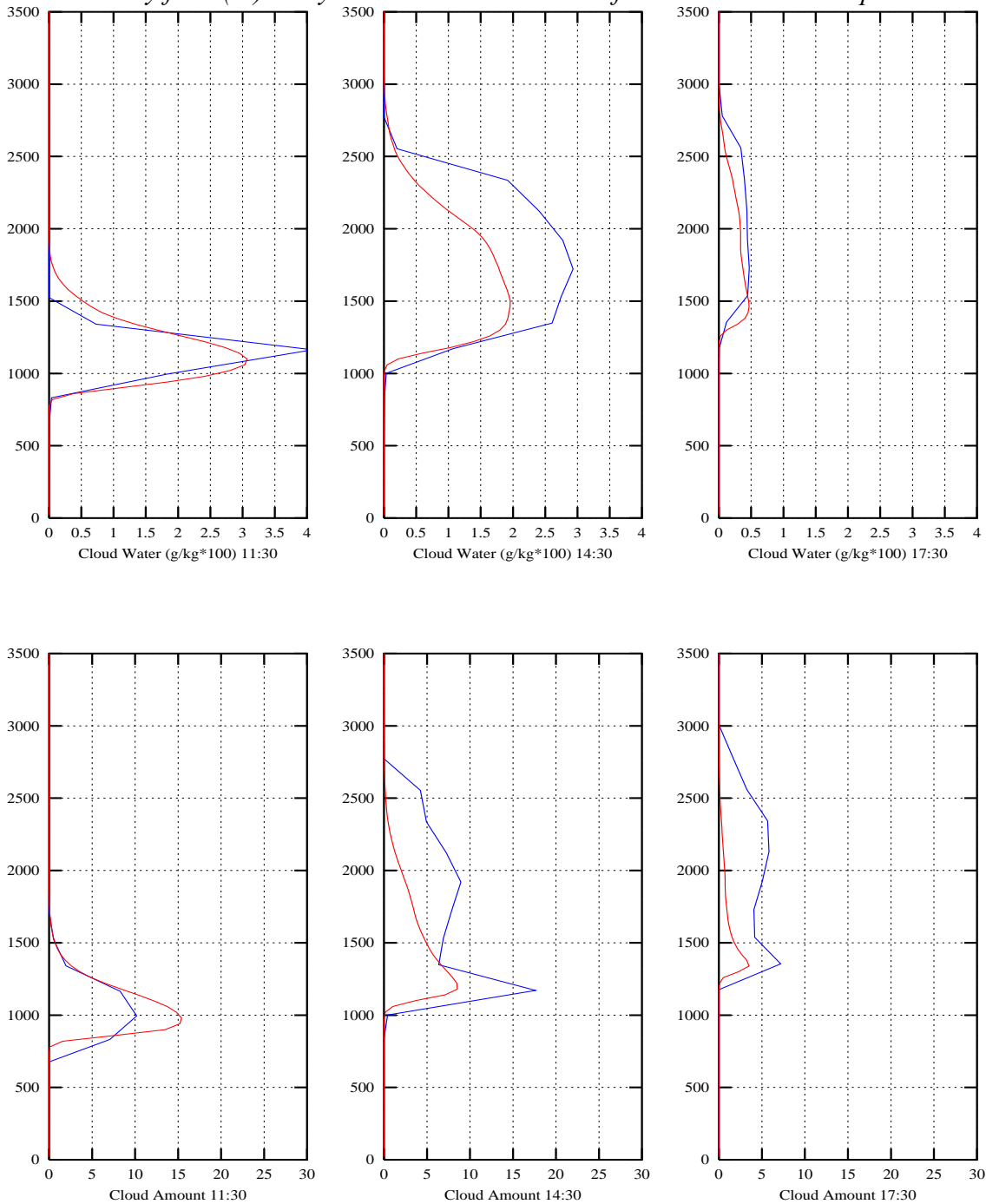


Figure 4: Evolution of mean thermodynamic profiles in RCA\_Albrecht and KNMI\_LES experiments. Blue is RCA, Red LES and Green the initial profiles. Top row shows evolution of

*potential temperature (in Kelvin), middle row total water field (in g/kg) and bottom row the relative humidity field (%). Only the lowest 3500 metres of the model domain is plotted.*



*Figure 5: Evolution of the vertical cloud fields in RCA\_Albrecht and KNMI\_LES models. Top row shows the cloud water field in g/kg\*100 at 11:30, 14:30 and 17:30. Bottom row shows the vertical profile of the cloud fraction. Blue is RCA\_Albrecht, Red is the KNMI\_LES.*

Figure 5 shows the evolution of the vertical cloud profiles through the simulated day. The same time periods and meaning as in figure 4 are applied to the RCA results. The top panel in figure 5 shows the evolution of the cloud water field and the lower panel the vertical cloud fraction (similar results for other single column models in the EUROCS project can be found

at <http://www.knmi.nl/samenw/eurocs>). Comparison is again made to the KNMI\_LES results. RCA develops a deepening cloud through the early afternoon, which thins with respect to cloud water amounts as one enters the early evening (17:30 profile). The reduced cloud water amounts result from a combination of the surface fluxes decreasing through the day (see Brown et al 2001 their figure 3 for the specified surface fluxes) and the deeper, higher cloud that boundary layer mixing must maintain as the day progresses. The RCA model shows a very reasonable evolution of the cloud water profile through the day. The cloud fraction profile also shows the correct evolution and vertical structure but does not decrease through the afternoon and evening as is seen in the LES model.

Many of the problems in modelling shallow cumulus clouds can be traced to assumptions made in the convective parameterisation schemes. In particular, details determining the rate of entrainment of environmental air into ascending cloudy plumes and the detrainment of cloud air into the environment, can strongly influence the simulated cloud and thermodynamic profiles. Siebsma and Cuijpers (1995) analysed the parametric assumptions made in the ECMWF and U.K. Met Office convection schemes (see Tiedtke 1989 and Gregory & Rowntree 1990 for details of the respective schemes) for entrainment and detrainment. They compared the entrainment and detrainment rates to those derived from LES simulations and concluded the parameterised rates were an order of magnitude in error. The rates of entrainment and detrainment, into and out of an ascending cloudy plume, will determine the cloud mass flux profile and cloud depth. They will also strongly influence the thermodynamic characteristics of the simulated cloud and, through detrainment, the moistening of the surrounding environment. Unfortunately, observations of entrainment and detrainment rates do not exist. One must therefore resort to comparison with LES models in an attempt to constrain parametric assumptions in convection schemes. Here we present an initial comparison of the RCA entrainment and detrainment rates with those derived from LES results published in Brown et al (2001) and Siebsma & Cuijpers (1995). Figure 6 presents the detrainment rates (top row), entrainment rates (middle row) and cloud mass flux (bottom row) in the RCA model at 12:30 and 14.30 local time. Also shown for comparison, are the LES inter-model mean entrainment rates and cloudy mass fluxes replotted from the Brown et al results. Both in RCA and the LES results, the cloud mass flux is seen to maximise close to cloud base and decrease with height through the cloud layer. In RCA this results from the fact that the detrainment rate is systematically larger than the entrainment rate (compare the top row in figure 6 to the middle row). This difference increases with depth through the cloud. The nett result of the detrainment/entrainment couplet is that the cloud mass flux decreases with height above cloud base. This profile is supported in the LES results and in the results of Siebsma & Cuijpers (1995). In particular, the occurrence of massive terminal detrainment at cloud top, associated with an increasing cloud mass flux with height, is avoided in RCA. This is important for the thermodynamic profiles in RCA and allows the potential temperature and relative humidity profiles to stay close to the LES results, even at cloud top. Likewise, the correct fractional relationship between entrainment and detrainment means the incloud thermodynamic state and buoyancy is reasonable in RCA. This is, in large part, the reason the vertical structure of cloud water in the RCA clouds is successfully simulated.

The entrainment rates in RCA appear around 2-3 times those simulated in the LES models (middle panel figure 6). The LES results reported in Brown et al (2001) are for cloudy core regions in the LES, we multiply these by 1.75 to get an approximate updraft entrainment rate. This factor is derived from the relationship between core entrainment rates and updraft entrainment rates presented in figure 11 of Siebsma and Cuijpers (1995) for BOMEX trade cumuli. We recognise that the LES derived updraft entrainment rates are extremely

approximate, but we feel the difference to RCA is probably a reliable conclusion. Siebsma & Cuijpers further indicate that in the BOMEX trade cumuli simulations the detrainment rates are around 1.5 times the fractional entrainment rates. This relationship appears to be reproduced to a first order in RCA. There is the suggestion, in the results in figure 6, that the RCA cloud mass flux penetrates higher than in the LES results. This tendency will occur if the detrainment/entrainment ratio is too small in the lower part of the cloud (too little detrainment relative to entrainment) and will lead to excessive cloud mass flux and detrainment in the upper portion of the cloud. With little direct verification data, we believe this is the case in RCA. The resulting excess detrainment and mass flux in the upper portion of the cloud and deficient mass flux and detrainment in the lower portion will lead to the convective tendencies of temperature and moistening being overestimated in the upper section of the clouds and underestimated in the lower section. These errors will lead to the vertical profile errors seen in figure 5 in the potential temperature and relative humidity fields through the cloud layer.

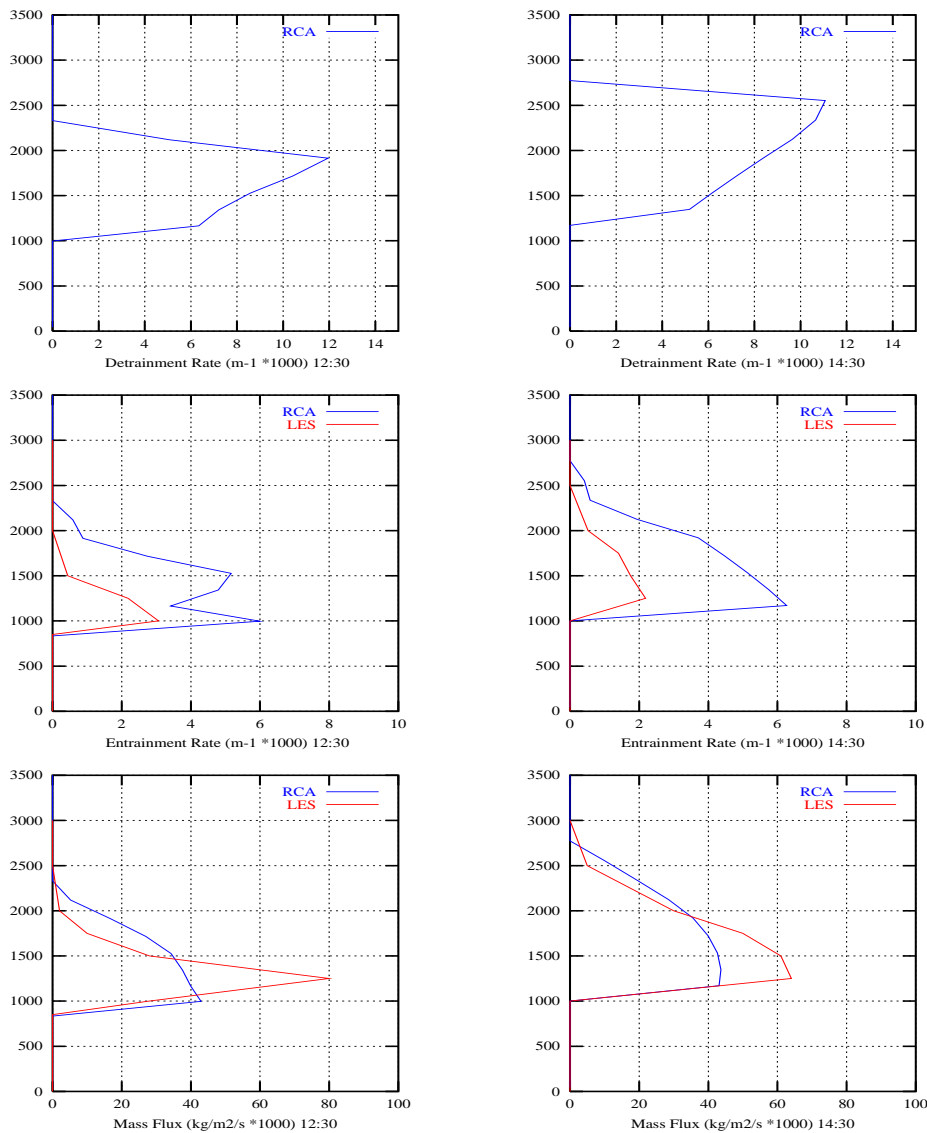


Figure 6: Top Row: RCA detrainment rates ( $m^{-1} * 1000$ ). Middle row: Modelled Entrainment Rates ( $m^{-1} * 1000$ ), blue is RCA and red is LES updraft entrainment rates derived from Brown

*etal (2001). Bottom Panel: Modelled Cloud Updraft Mass flux ( $\text{kgm}^{-2}\text{s}^{-1}$ ), blue is RCA, red is LES results from Brown etal (2001). Plots are for 12:30 and 14:30.*

RCA assumes a cloud radius of 300m for the bulk cloud model used in the shallow convection calculations. Siebsma and Cuijpers (1996) and Nitta (1975) suggest, both from LES and observations during BOMEX, that the dominant cloud size in the spectrum of clouds is around 100m. An overestimate of the cloud radius will lead to a direct overestimate of the entrainment and detrainment rates in RCA, as seen in figure 6. But, the large cloud radius will also mean the thermodynamic effect of entrained air on the buoyancy of cloud parcels will be underestimated. As entrainment and detrainment are determined through the buoyancy sorting method, this can result in an excessive number of buoyant admixtures in the lower section of the cloud layer and a relative ratio of entrainment to detrainment that is too high in the lower half of the cloud. As a result the cloud mass flux will not decrease sufficiently rapidly with height above cloud base.

## 5. Conclusions

We have analysed the representation of land based shallow cumulus convection in the RCA model. For this particular day of shallow cumulus convection over the ARM SGP site, RCA produces a very realistic description of the shallow cumulus cloud diurnal cycle. The onset of shallow convection was slightly later than seen in the LES models and is likely related to details of the convective trigger function applied to determine the onset of convection. Nevertheless, the timing of onset was relatively well simulated, as was the decay of the cloud field. The gross measures of the cloud field, namely cloud fraction and cloud water were well represented as were the evolution of the model thermodynamic profiles, when compared to LES results. There was a clear tendency for the RCA model to mix too deeply in the vertical, with a dry bias in the lower portion of the cloud field and a moist bias in the upper portion when compared to the LES model. It was indicated that this may be related to the relative magnitudes of entrainment and detrainment rates through the cloud, resulting in a cloud mass flux that does not decrease sufficiently rapidly with height. It was further suggested that the thermodynamic effect of, in particular the parameterised entrainment, on the cloud plume thermodynamics may be underestimated because the specified cloud radius is larger than seen in observations and LES models. Observations to support this and to constrain the entrainment and detrainment terms are extremely rare. Further comparison, using other cases, against LES models is likely the best avenue for parameterisation development. Nevertheless, the overall relationship between cloud entrainment and detrainment rates appears to mimic LES results leading to a reasonably realistic vertical profile of cloud mass flux.

Finally a new parameterisation of the shallow cumulus cloud fraction has been introduced into RCA. This links the shallow cumulus cloud fraction more directly to shallow cumulus updrafts and therefore the subcloud layer. Results using this new parameterisation, show that the modelled cloud water field and resulting surface solar radiation flux are very sensitive to the method by which the shallow cumulus cloud fraction is calculated. In the RCA model, failure to model this field of shallow cumulus clouds would lead to an overestimate of the surface solar radiation by  $\sim 40\text{Wm}^{-2}$ , as a daily mean value. These types of errors can lead to serious seasonal mean errors in key surface variables in climate models and indicate the importance of accurately representing land based shallow convection and the associated cloud-radiation effects.

## Acknowledgements

Geert Lenderink and Pier Siebesma (KNMI) developed the forcing data sets used in this study, for the EUROCS project. Roel Neggers and Pier Siebesma (KNMI) performed the KNMI LES simulations of the case, used for evaluation within this article. This work was funded under the EU Framework V project EUROCS (EVK2-CT-1999-00051)

## References

- Albrecht B. 1981: Parameterisation of Trade Cumulus Cloud Amounts: *Journal of Atmos Sci.* 38, 97-105.
- Betts A.K. 1997: Trade Cumulus: Observations and Modelling. In *The Physics and Parameterisation of Moist Atmospheric Convection*. Editor: R.K.Smith. *NATO ASI Series C, Volume 505*. Kluwer Academic Publishers.
- Blyth A.M. W.A Cooper and J.B.Jensen 1988: A study of the source of entrained air in Montana cumuli. *Journal of Atmos. Sci.* 45, 3944-3964
- Brown A, R.T. Cederwall, A.Chlond, P.G.Duynkerke, J-C Golaz, M.Khairoutdinov, D.C. Llewellyn, A.P.Lock, M.K.MacVean, C-H Moeng, R.A.J Neggers, A.P.Siebsema and B.Stevens 2002: Large-eddy simulation of the diurnal cycle of shallow cumulus convection over land. Accepted for publication *Q.J.R Meteorol. Soc.* 2002.
- Cuxart J., P. Bougeault and J.L. Redelsperger 2000. A turbulence scheme allowing for mesoscale and large eddy simulations. *Q.J.R Meteorol. Soc* 126 1-30.
- Emanuel K.A. 1994: Atmospheric Convection. *Oxford University Press*
- Fritsch M.J and C.F. Chappell 1980: Numerical Prediction of convectively driven mesoscale pressure systems: Part I Convective Parameterisation. *Journal of Atmos Sci* 37, 1722-1733
- Gregory D and P.R. Rowntree 1990: A mass flux scheme with representation of cloud ensemble characteristics and stability dependent closure. *Mon. Wea. Rev.* 118, 1483-1506.
- Kain J.S and M.J.Fritsch 1990: A One-Dimensional Entraining/Detraining Plume Model and its application in Convective Parameterisation. *Journal of Atmos Sci.* 47, 2784-2802
- Jones C.G. 2001: A brief description of RCA2 (The Rossby Centre Atmosphere Model Version 2). In *SWECLIM Newsletter* 11, 9-14. Available from Rossby Centre, SMHI, Norrköping.
- Nitta Ts. 1975: Observational determination of cloud mass flux distributions. *Journal of Atmos Sci.* 32, 73-91
- Rasch P. And Kristjansson J.E. 1998: A comparison of the CCM3 model climate using diagnosed and predicted condensate parameterisations. *J.Climate* 12, 531-539.

Siebsma A.P and J.W.M Cuijpers 1995: Evaluation of parametric assumptions for shallow cumulus convection. *Journal of Atmos Sci.* 52, 650-666.

Slingo J. 1987: The development and verification of a cloud prediction scheme for the ECMWF model. *Q.J.R. Meteorol. Soc* 113, 89-928

Tiedtke M. 1989: A comprehensive mass flux scheme for cumulus parameterisation in large scale models. *Mon. Wea. Rev.* 117, 1779-1800

Xu K-M and S.Krueger 1991: Evaluation of cloudiness parameterisations using a cumulus ensemble model. *Mon. Wea. Rev.* 119, 342-367.